

## Substituent-Control Exciton in J-Aggregates of Protonated Water-Insoluble Porphyrins

Shinsuke Okada<sup>†</sup> and Hiroshi Segawa<sup>\*†‡</sup>

Contribution from the Department of Applied Chemistry, Graduate School of Engineering, and Department of Chemistry, Graduate School of Arts and Sciences, The University of Tokyo, 3-8-1 Komaba, Meguro-ku, Tokyo 153-8902, Japan

Received December 14, 2001; E-mail: csegawa@mail.ecc.u-tokyo.ac.jp

**Abstract:** A series of protonated porphyrin J-aggregates of various water-insoluble tetraphenylporphyrin derivatives was prepared by aggregation at the liquid–liquid or gas–liquid interface. Using atomic force microscopy, we observed microcrystalline porphyrin J-aggregates. The J-aggregates have two strong exciton bands corresponding to the B (Soret)- and Q-bands of the protonated porphyrin. Interestingly, the excitation energy of the lower exciton (denoted by S1) markedly depends on the *meso*-substituents, whereas that of the higher exciton (denoted by S2) does not depend on them. These results indicate that the nature of the exciton coupling of the S1 transition dipole moment can be systematically changed by the substituents.

### Introduction

Porphyrin aggregates<sup>1,2</sup> have been investigated in connection with the functions of chlorophyll aggregates in photosynthetic organisms in plants and bacteria.<sup>3</sup> Because the natural chlorophyll aggregates in the light-harvesting proteins or chlorosomes have a strong transition dipole moment aligned in the “head-to-tail” direction,<sup>3</sup> porphyrin J-aggregates<sup>4</sup> are important for the study of the excited-state model of the organisms. However, the porphyrin J-aggregates reported to date are limited to water-soluble tetraphenylporphinesulfonate (TSPP)<sup>4a–g</sup> and a specific picket-fence porphyrin;<sup>4i</sup> therefore, there are no variations in the J-aggregates, which are necessary for investigating changes in the interaction and the photophysical properties that are

important for the elucidation of the molecular exciton on porphyrin assembly. To construct the various J-aggregates from the water-insoluble porphyrin derivatives, “interfacial aggregation”<sup>4i</sup> is considered to provide a useful methodology. In fact, an important sign suggesting the J-aggregate formation of protonated tetraphenylporphyrin that is adsorbed at the toluene–aqueous sulfuric acid interface was reported on the external reflection spectrum;<sup>5</sup> however, the J-aggregate has not yet been isolated. If the liquid–liquid or the gas–liquid interfacial formation can be applied to various water-insoluble porphyrins to obtain isolated porphyrin J-aggregates, new studies will soon be conducted on biological aspects and material applications. With this in mind, we constructed several varieties of the porphyrin J-aggregate from a series of water-insoluble porphyrin derivatives.

### Results and Discussion

**Aggregation in Emulsion.** A series of the free base tetraphenylporphyrin derivatives used here (Figure 1) was prepared by standard procedures.<sup>6</sup> To construct the stable J-aggregate under ambient temperature, the condition of the solvent and the aqueous acid is important. When a few drops of concentrated sulfuric acid are added to the free base porphyrin solutions of CH<sub>2</sub>Cl<sub>2</sub>, typical protonation of the inner nitrogen in the porphyrin rings is observed in all cases, but no aggregate is formed. On the other hand, when aqueous sulfuric acid is added to the CH<sub>2</sub>Cl<sub>2</sub> solutions, emulsion with aggregate assembly is obtained. The typical absorption change of tetraphenylporphyrin (TPP) in emulsion with an increasing concentration of the aqueous sulfuric acid from 0 to 20% (w/w) is shown in Figure 2. After a few drops of sulfuric acid (20% (w/w)) were added

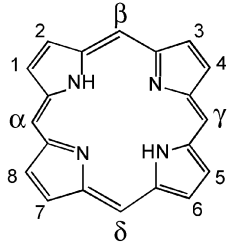
<sup>†</sup> Graduate School of Engineering.

<sup>‡</sup> Graduate School of Arts and Sciences.

- (1) (a) White, W. I. In *The Porphyrins*; Dolphin, D., Ed.; Academic Press: New York, 1979; Vol. V, Chapter 7, pp 303–339. (b) Katz, J. J.; Shipman, L. L.; Cotton, T. M.; Janson, T. R. In *The Porphyrins*; Dolphin, D., Ed.; Academic Press: New York, 1979; Vol. V, Chapter 9, pp 401–458. (c) Hambright, P. In *The Porphyrin Handbook*; Kadish, K. M., Smith, K. M., Guillard, R., Eds.; Academic Press: New York, 2000; Vol. 3, Chapter 18, pp 129–210.
- (2) Pasternack, R. F.; Huber, P. R.; Boyd, P.; Engasser, G.; Francesconi, L.; Gibbs, E.; Fasella, P.; Venturo, G. C.; Hinds, L. de C. *J. Am. Chem. Soc.* **1972**, *94*, 4511–4517.
- (3) (a) Deisenhofer, J.; Epp, O.; Miki, K.; Huber, R.; Michel, H. *Nature* **1985**, *318*, 618–624. (b) McDermott, G.; Prince, S. M.; Freer, A. A.; Hawthornthwaite-Lawless, A. M.; Papiz, M. Z.; Cogdell, R. G.; Isaacs, N. W. *Nature* **1995**, *374*, 517–521. (c) Karrasch, S.; Bullough, P. A.; Gosh, R. *EMBO J.* **1995**, *14*, 631–638. (d) Koepke, J.; Hu, X.; Muenke, C.; Schulten, K.; Michel, H. *Structure* **1996**, *4*, 581–597. (e) Olson, J. M. *Photochem. Photobiol.* **1998**, *67*, 61–75.
- (4) (a) Ohno, O.; Kaizu, Y.; Kobayashi, H. *J. Chem. Phys.* **1993**, *99*, 4128–4139. (b) Ribo, J. M.; Crusats, J.; Farrera, J.-A.; Valero, M. L. *J. Chem. Soc., Chem. Commun.* **1994**, 681–682. (c) Pasternack, R. F.; Schaefer, K. F.; Hambright, P. *Inorg. Chem.* **1994**, *33*, 2062–2065. (d) Akins, D. L.; Zhu, H.-R.; Guo, C. *J. Phys. Chem.* **1994**, *98*, 3612–3618. (e) Maiti, N.; Ravikanth, M.; Mazumdar, S.; Periasamy, N. *J. Phys. Chem.* **1995**, *99*, 17192–17197. (f) Akins, D. L.; Özçelik, S.; Zhu, H.-R.; Guo, C. *J. Phys. Chem.* **1996**, *100*, 14390–14396. (g) Akins, D. L.; Zhu, H.-R.; Guo, C. *J. Phys. Chem.* **1996**, *100*, 5420–5425. (h) Jin, R.-H.; Aoki, S.; Shima, K. *J. Chem. Soc., Faraday Trans.* **1997**, *93*, 3945–3953. (i) Barber, D. C.; Freitag-Beeston, R. A.; Whitten, D. G. *J. Phys. Chem.* **1991**, *95*, 4074–4086.

(5) Moriya, Y.; Amano, R.; Sato, T.; Nakata, S.; Ogawa, N. *Chem. Lett.* **2000**, 556–557.

(6) Adler, A. D.; Longo, F. R.; Finarelli, J. D.; Goldmacher, J.; Assour, J.; Korsakoff, L. *J. Org. Chem.* **1967**, *32*, 476.



abbreviation	meso-substituent ( $\alpha, \beta, \gamma, \delta$ )	$\beta$ -substituent (1,2,3,4,5,6,7,8)
porphine	H	H
OEP	H	-CH <sub>2</sub> CH <sub>3</sub>
TPP		H
TThP		H
T(4-NO <sub>2</sub> )P		H
T(4-CN)P		H
T(4-MeOP)P		H
T(4-BuOP)P		H
T(3,5-MeOP)P		H
T(2,4,6-MeP)P		H

**Figure 1.** Structures and abbreviations of free base porphyrins used in this study.

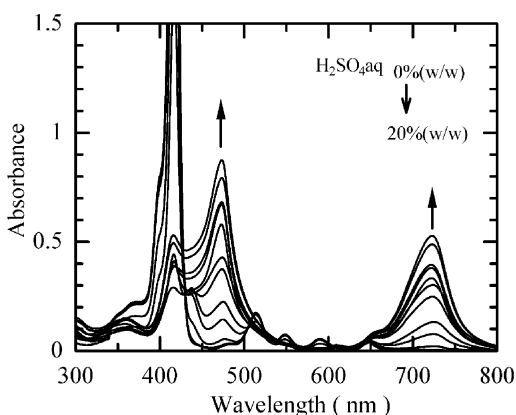


**Figure 2.** Absorption changes of TPP ( $10^{-5}$  M) in an emulsion of CH<sub>2</sub>Cl<sub>2</sub>–water with increasing concentrations of aqueous sulfuric acid: 0, 2.0, 5.0, 8.0, 8.9, 12, 13.3, 14.5, 16.7, 17.1, 18.5, and 20% (w/w).

to 200  $\mu$ L of a  $10^{-5}$  M porphyrin–CH<sub>2</sub>Cl<sub>2</sub> solution, the B-band of the free base monomer (417 nm) was first replaced by an absorption at 438 nm (protonated monomer); a new absorption then appeared at 475 nm. Simultaneously, a new Q-band appeared at 725 nm, which is a considerably longer wavelength than that of a protonated monomer (652 nm). The red-shifted absorption peaks signify that the assembly consists of the “head-to-tail” aggregates (J-aggregates). Under the stationary condition, phase separation is observed. In this case, stable assembly accumulates at the interface.

The stable interface assembly was not formed when hydrochloric acid or nitric acid was used. Therefore, sulfate anion seems to act not only as a counterion but also as an important element interacting with the porphyrin J-aggregates. It is well

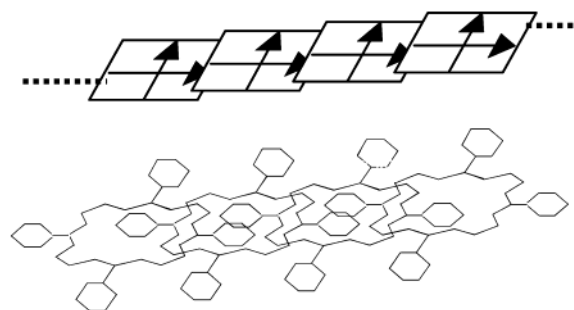


**Figure 3.** Proposed structure of the porphyrin J-aggregate.

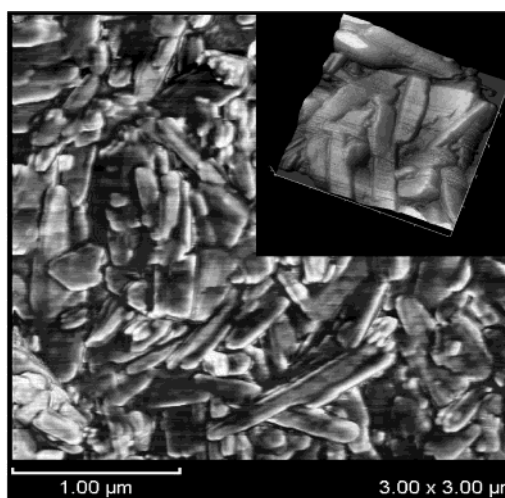


**Figure 4.** AFM image ( $3 \mu\text{m} \times 3 \mu\text{m}$ , tapping mode, phase imaging) of a T(4-CNP)P J-aggregate on a glass substrate. The inset shows a 3D topographic image ( $1 \mu\text{m} \times 1 \mu\text{m}$ ).

known that the sulfate anion tightly binds water molecules. The role of the sulfate anion should be considered in relation to both the electrostatic interaction and the network structure with water molecules and protonated porphyrin from the standpoint of overall thermodynamic stability.

The porphyrins substituted at the 2,6 or 3,5 positions of *meso*-phenyl groups did not form J-aggregates. It is considered that these substituents prevent porphyrins from forming aggregates by steric hindrance. Except for the steric hindrance, all of the porphyrins with aromatic rings at the *meso*-position of porphyrin rings formed J-aggregates, whereas OEP and porphine did not. Including the water-soluble porphyrin J-aggregates reported to date, the aromatic rings at the *meso*-position are considered to be necessary for the formation of porphyrin J-aggregates. As the proposed structure of the TSPP J-aggregate,<sup>4b,e,g</sup> the peripheral rigid phenyl groups can stabilize the slipped face-to-face structure as shown in Figure 3.

**J-Aggregate Formed at the Liquid–Liquid Interface.** The J-aggregate assembly that was slowly growing at the interface for an hour was stable enough to be placed on a glass substrate and taken out of the solution. The typical AFM image of the J-aggregate film on the glass substrate is shown in Figure 4. In many cases, square rodlike microcrystals are observed, although the microcrystal structure is dependent on the *meso*-substituents and the growing conditions.

Figure 5 shows several transmission absorption spectra of the film on the glass substrate. The absorption spectra of the J-aggregates on the glass substrates were relatively broad as compared to those of the water-soluble porphyrin J-aggregate,<sup>4</sup>

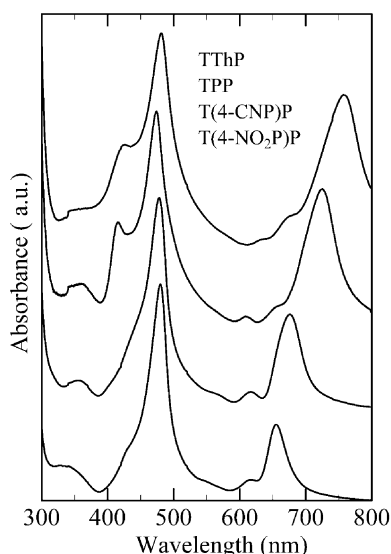


**Figure 5.** Transmission absorption spectra of several tetraphenylporphyrin J-aggregates formed at the liquid–liquid interface.

**Table 1.** Absorption Maxima (nm) of the Free Base, Acid Dication, and J-Aggregate of the Porphyrins

porphyrin	free base		acid dication		J-aggregate	
	Soret	Q <sup>a</sup>	Soret	Q <sup>b</sup>	Soret	Q <sup>b</sup>
T(4-NO <sub>2</sub> )P	423	645	447	650	480	658
T(4-CNP)P	420	645	443	650	478	676
TPP	417	646	438	652	475	725
TThP	420	652	447	678	481	756
T(4-MeOP)P	421	650	451	685	486	753
T(4-BuOP)P	422	651	452	687	481	761
T(3,5-MeOP)P	420	645	451	653	n.d.	n.d.
T(2,4,6-MeP)P	419	646	435	631	n.d.	n.d.
OEP	397	619	406	593	n.d.	n.d.
porphine	392	614	402	547	n.d.	n.d.

<sup>a</sup> Q<sub>x</sub>(0–0). <sup>b</sup> Q(0–0).

suggesting the occurrence of an incoherent interaction in the surroundings of the dense film. Furthermore, the fwhm of the Q-band absorption increased with an increase in the electron-donating character of the *meso*-substituents. Interestingly, the Q-band absorption peaks of the J-aggregates vary widely from 658 to 756 nm despite the fact that all of the B-bands are seen at around 480 nm (Table 1). Obviously, the excitation energy of the S1 exciton estimated from the absorption peaks depends on the *meso*-substituents. This seemed to be in agreement with the degree of electron-donating properties of the *meso*-substituents, where electron-withdrawing substituents (e.g., –NO<sub>2</sub> or –CN) cause a small energy shift, and electron-releasing substituents (e.g., –OMe or –OBU) cause a large energy shift (Figure 6).

In the cases of the free base and the acid dications of the tetraphenylporphyrin derivatives, increasing bathochromic shifts and increasing transition dipoles of the Q-band were observed with an increase in the electron-donating power of the substituents.<sup>7</sup> In the case of the J-aggregates, the trend is similar, but the effect is quite large. The strong substituent effect on the Q-band is considered to be due to not only a resonance effect through the raising of a<sub>2u</sub> HOMO by the electron-donating *meso*-substituents but also an enhancement of the transition dipole through the degeneracy of the a<sub>1u</sub> and the a<sub>2u</sub> orbitals. In fact,

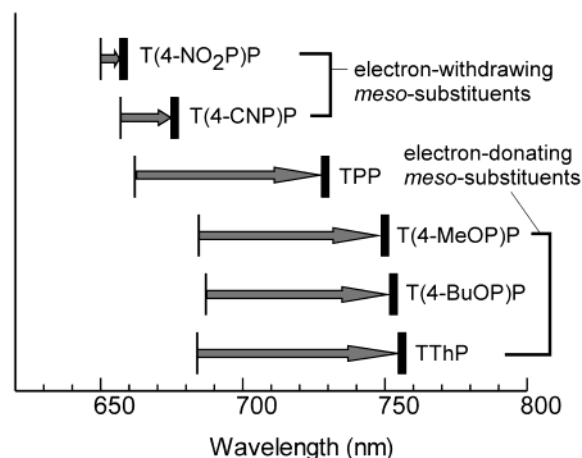


**Figure 6.** Absorption energy shifts of several tetraphenylporphyrin J-aggregates from the corresponding acid dications.

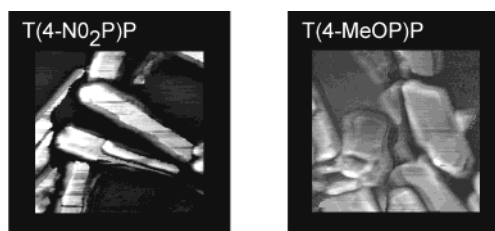


**Figure 7.** AFM images (0.5 μm × 0.5 μm, tapping mode, phase imaging) of T(4-NO<sub>2</sub>)P J-aggregate (left) and T(4-MeOP)P J-aggregate (right) on glass substrate.

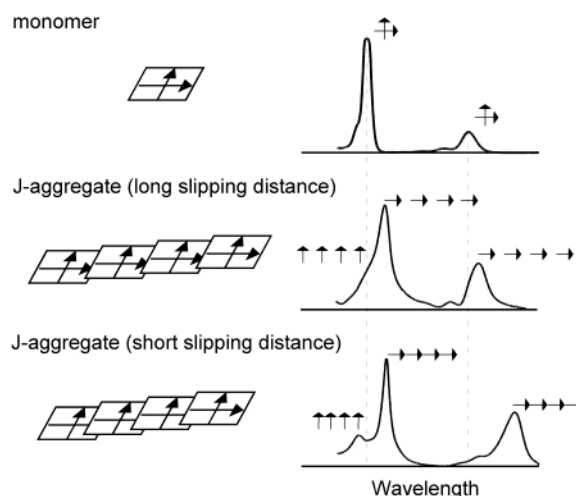


**Figure 8.** Schematic relationship between the slipping distance and the absorption feature of the porphyrin J-aggregate.

the relative absorbance of the Q-band to the B-band increased with an increase in the electron-donating character of the *meso*-substituents (Figure 5). However, the total spectral features cannot be explained by the electron-donating character of the substituents alone. For a full explanation, the directional change of the transition dipole aligned with the aggregation axis and/or the conformational change of the local stacking structure should also be taken into account. For instance, the higher energy absorption shoulder of the B-band assigned to the orthogonal transition dipoles to the aggregation axis also depended on the *meso*-substituents (Figure 5), indicating the structural change of the J-aggregates. In careful AFM measurements, the *meso*-substituent dependences of the exterior shapes

(7) Meot-Ner, M.; Adler, A. D. *J. Am. Chem. Soc.* **1975**, *97*, 5107–5111.

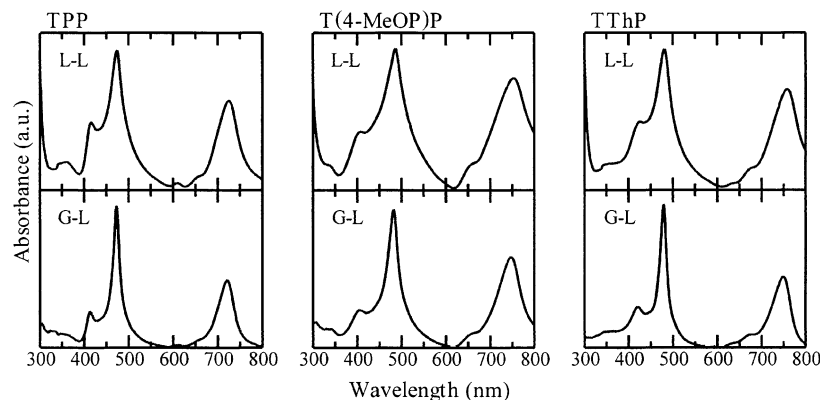


**Figure 9.** Absorption spectra of several porphyrin J-aggregates formed at the liquid–liquid (L–L) and gas–liquid (G–L) interfaces.

of the J-aggregate microcrystals were observed (Figure 7). In the case of T(4-MeOP)P J-aggregates, square and lamellar structures were observed, suggesting that the one-dimensional slipping distance of the J-aggregate decreased. Although the large difference of the Q-band shifts of the J-aggregates conflicts with the small difference of the Q-bands of the acid dications, the “substituent-dependent slipping distance” of the J-aggregates could rationalize the total absorption features. The possible relationship between the slipping distance and the absorption feature of the porphyrin J-aggregates is described in Figure 8. The short slipping distance causes the higher energy absorption of the B-band, whereas the long slipping distance does not. This is consistent with the large energy shifts of the Q-band of T(4-MeOP)P.

**Aggregation at the Air–Water Interface.** The water-insoluble porphyrin J-aggregates can also be formed by the use of an air–water interface. Dropping the porphyrin–CH<sub>2</sub>Cl<sub>2</sub> solution on the surface of aqueous sulfuric acid leads to J-aggregate formation at the interface after the solvent evaporation. The absorption spectra of the J-aggregates formed at the air–water interface (Figure 9) show relatively sharp absorption bands as compared to those of the J-aggregates formed at the liquid–liquid interface.

These results suggest a less incoherent interaction in the J-aggregate films than that formed at the liquid–liquid interface, where the porphyrin molecules assemble toward a three-dimensional crystal from the CH<sub>2</sub>Cl<sub>2</sub> solution. In the case of the T(4-CNP)P, the J-aggregates at the air–liquid interface have sharp but split S<sub>2</sub> exciton bands at 470 and 482 nm, indicating that some polymorphism may exist in these J-aggregate microcrystals. It is noteworthy that the absorption peak energies of the J-aggregates formed at the gas–liquid interface are almost identical to those formed at the liquid–liquid interface. These results indicate that the energy levels of the S<sub>1</sub> exciton of the porphyrin J-aggregates are of intrinsic character depending on the substituents. In other words, the strength of the exciton coupling of the S<sub>1</sub> transition dipole moment can be systematically changed by the substituents, by which strong, medium, and weak coupling can be accomplished in the porphyrin J-aggregates.

## Conclusion

In conclusion, interface, sulfuric acid, and aromatic rings at the *meso*-position are needed for stable J-aggregate formation. The absorption peak shifts suggest that the energy levels of the

S<sub>1</sub> exciton of the porphyrin J-aggregates depend on the substituents. The energetically tunable exciton of S<sub>1</sub> will facilitate the clarification of the exciton characteristics of porphyrin assembly through a systematic study of their excited state, which might serve for a better understanding of the functions of chlorophyll aggregates in photosynthetic organisms. Additional photophysical properties and structural determination are under investigation.

## Experimental Section

The free base tetraphenylporphyrin derivatives used in this study (Figure 1) were prepared by standard procedures,<sup>6</sup> except for *meso*-tetra(3,5-methoxyphenyl)porphyrin (T(3,5-MeOP)P), which was purchased from Tokyo KASEI. Porphine and octaethylporphyrin (OEP) were purchased from Porphyrin Products, Inc.

Glass substrates were used after immersion in CH<sub>2</sub>Cl<sub>2</sub> for a few days. The absorption spectra of the porphyrin solution and the J-aggregates on the glass substrate were recorded using a UV/VIS/NIR spectrophotometer (JASCO, V-570). The AFM images of the J-aggregates on the glass substrate were recorded using a scanning probe microscope (Shimadzu, SPM-9500J3, tapping-mode AFM). <sup>1</sup>H NMR spectra were taken using an FT-NMR spectrometer (JEOL, JMA-A500, 500 MHz).

***meso*-Tetraphenylporphyrin (TPP).** <sup>1</sup>H NMR (CDCl<sub>3</sub>, TMS): δ 8.85 (s, 8H, βH), 8.22 (d, 8H, *J*<sub>H–H</sub> = 7.6 Hz, *o*-*meso*-phenyl-H), 7.76 (m, 12H, *m*-*meso*-phenyl-H, *p*-*meso*-phenyl-H), –2.77 (s, 2H, N–H).

***meso*-Tetra(2-thienyl)porphyrin (TThP).** <sup>1</sup>H NMR (CDCl<sub>3</sub>, TMS): δ 8.98 (s, 8H, βH), 8.01 (m, 8H, thienyl-3H, thienyl-4H), 7.74 (dd, 4H, *J*<sub>H–H</sub> = 4.3 Hz, thienyl-5H), –2.75 (s, 2H, N–H).

***meso*-Tetra(4-nitrophenyl)porphyrin (T(4-NO<sub>2</sub>)P).** <sup>1</sup>H NMR (C<sub>5</sub>D<sub>5</sub>N, TMS): δ 9.19 (s, 8H, βH), 8.68 (d, 8H, *J*<sub>H–H</sub> = 8.7 Hz, *o*-*meso*-phenyl-H), 8.55 (d, 8H, *J*<sub>H–H</sub> = 8.7 Hz, *m*-*meso*-phenyl-H), –2.56 (s, 2H, N–H).

***meso*-Tetra(4-cyanophenyl)porphyrin (T(4-CNP)P).** <sup>1</sup>H NMR (CDCl<sub>3</sub>, TMS): δ 8.80 (s, 8H, βH), 8.33 (d, 8H, *J*<sub>H–H</sub> = 8.2 Hz, *o*-*meso*-phenyl-H), 8.10 (d, 8H, *J*<sub>H–H</sub> = 8.2 Hz, *m*-*meso*-phenyl-H), –2.88 (s, 2H, N–H).

***meso*-Tetra(4-methoxyphenyl)porphyrin (T(4-MeOP)P).** <sup>1</sup>H NMR (CDCl<sub>3</sub>, TMS): δ 8.86 (s, 8H, βH), 8.13 (d, 8H, *J*<sub>H–H</sub> = 8.6 Hz, *o*-*meso*-phenyl-H), 7.29 (d, 8H, *J*<sub>H–H</sub> = 8.6 Hz, *m*-*meso*-phenyl-H), 4.10 (s, 12H, p-OCH<sub>3</sub>), –2.75 (s, 2H, N–H).

***meso*-Tetra(4-butoxyphenyl)porphyrin (T(4-BuOP)P).** <sup>1</sup>H NMR (CDCl<sub>3</sub>, TMS): δ 8.86 (s, 8H, βH), 8.11 (d, 8H, *J*<sub>H–H</sub> = 8.6 Hz, *o*-*meso*-phenyl-H), 7.27 (d, 8H, *J*<sub>H–H</sub> = 8.6 Hz, *m*-*meso*-phenyl-H), 4.26–1.10 (36H, *p*-BuO), –2.75 (s, 2H, N–H).

***meso*-Tetra(2,4,6-methylphenyl)porphyrin (T(2,4,6-MeP)P).** <sup>1</sup>H NMR (CDCl<sub>3</sub>, TMS): δ 8.61 (s, 8H, βH), 7.27 (s, 8H, *m*-*meso*-phenyl-

H), 2.62 (s, 12H, *p*-*meso*-phenyl-CH<sub>3</sub>), 1.85 (s, 24H, *o*-*meso*-phenyl-CH<sub>3</sub>), -2.51 (s, 2H, N-H).

**Acknowledgment.** This work was supported by a Grant-in-Aid for Exploratory Research and Scientific Research on Priority Areas (417) from the Ministry of Education, Culture, Sports,

Science and Technology (MEXT) of the Japanese Government. The authors wish to thank Mr. Masao Matuda of the Shimadzu Co. for help in carrying out the AFM measurements.

JA017768J